Applied Catalysis B: Environmental 99 (2010) 289–297

Contents lists available at ScienceDirect

Applied Catalysis B: Environmental

journal homepage: www.elsevier.com/locate/apcatb

# Comparative study of alumina-supported transition metal catalysts for hydrogen generation by steam reforming of acetic acid

Xun Hu [a,b], Gongxuan Lu [a,*]

[a] State Key Laboratory for Oxo Synthesis and Selective Oxidation, Lanzhou Institute of Chemical Physics, Chinese Academy of Sciences, Lanzhou 730000, PR China
[b] Graduate School of Chinese Academy of Sciences, Beijing 100039, PR China

ARTICLE INFO

*Article history:*
Received 22 January 2010
Received in revised form 19 June 2010
Accepted 21 June 2010
Available online 26 June 2010

*Keywords:*
Acetic acid
Steam reforming
Hydrogen
$Ni/Al_2O_3$
$Co/Al_2O_3$

ABSTRACT

The reaction of acetic acid steam reforming for $H_2$ production has been investigated over transition metal catalysts (Ni, Co, Fe or Cu)/$Al_2O_3$. $Ni/Al_2O_3$ and $Co/Al_2O_3$ catalysts are active for acetic acid steam reforming while $Fe/Al_2O_3$ and $Cu/Al_2O_3$ catalysts present negligible activity. The difference can be attributed to the different cracking activity of the metals toward the C–C and C–H bonds of acetic acid molecule. Detailed comparisons in terms of catalytic activity, selectivity, and stability are carried out over $Ni/Al_2O_3$ and $Co/Al_2O_3$ catalysts. Distinct product distributions were observed between them. $CH_4$ production was favored over $Ni/Al_2O_3$ catalyst at mild temperatures while CO production was favored over $Co/Al_2O_3$ catalyst at high temperatures, which were induced by the different reaction networks over the two catalysts. Moreover, in the stability tests, $Ni/Al_2O_3$ catalyst was much more stable than $Co/Al_2O_3$ catalyst. Serious coke deposition and oxidation of metallic phase led to the fast deactivation of $Co/Al_2O_3$ catalyst. On the contrary, much slower coke formation rates and metal sintering rates as well as much higher resistivity of active metal toward oxidation guaranteed the stability of $Ni/Al_2O_3$ catalyst.



## 1. Introduction

Presently, production of hydrogen attracts great interest in energy area because of the potential application of hydrogen in fuel cells [1–6]. Most hydrogen now is produced from fossil-based materials. However, the environmental concerns associated with the fast depletion of fossil fuels reserves are increasingly demanding a clean and renewable hydrogen resource. Among the potential alternatives available, biomass is regarded as an appropriate energy resource due to its carbon-neutral nature and easy availability [7–12]. In general, the flash pyrolysis of biomass to bio-oil and the followed steam reforming is proposed as a viable way for hydrogen production [13–15]. Bio-oil is a complex mixture of organic compounds [16–18] and its steam reforming is characterized with lots of difficulties [19]. Steam reforming of the model components in bio-oil is much easier. Moreover, it can offer much information for preparing active catalysts and optimizing experimental conditions for steam reforming of a real bio-oil. Acetic acid is one of the main components in bio-oil [20] and a safe hydrogen carrier due to its non-inflammable nature. Because of these special characteristics, steam reforming of acetic acid has been widely performed by different research groups [21–36]. The catalysts employed in the works concentrated on Ni-based catalysts [21–30] and noble metal catalysts [30–34]. Basagiannis et al. studied the catalytic behaviors of several Ni and noble metal-based catalysts [29–31]. They found that Ni and Ru catalysts were more active and selective for hydrogen production. Complete conversion of acetic acid was observed at 1023 K, and only hydrogen and carbon oxides were produced as the main products. Galdamez et al. [26] investigated acetic acid steam reforming using a co-precipitated Ni–Al catalyst promoted with lanthanum at 923 K. The modification with lanthanum did not increase the $H_2$ yield achieved over Ni–Al catalyst. In addition, a bifunctional mechanism was proposed for steam reforming of acetic acid over $Pt/ZrO_2$ catalyst [32–34].

In our previous works [35,36], the effects of operating parameters on acetic acid reforming reactions were investigated in a detailed manner using two bimetallic catalysts: Fe–Co and Ni–Co. While in this study, the catalytic properties of $Al_2O_3$-supported Ni, Co, Fe, and Cu catalysts in acetic acid reforming reactions were explored in detail. In particular, the different catalytic behaviors between $Ni/Al_2O_3$ and $Co/Al_2O_3$ catalysts were focused. Nickel and cobalt were the most widely used transition metals for various steam reforming reactions, and both of them were suggested as suitable materials because of their superior catalytic performances [3,19]. However, the detailed comparisons of Ni and Co catalysts in terms of catalytic behaviors in acetic acid reforming reactions have not yet been reported. Besides, to our knowledge, the catalytic performances of $Co/Al_2O_3$, $Fe/Al_2O_3$, and $Cu/Al_2O_3$ catalysts in acetic

* Corresponding author. Tel.: +86 931 4968178; fax: +86 931 4968178.
*E-mail address:* gxlu@lzb.ac.cn (G. Lu).

0926-3373/$ – see front matter © 2010 Elsevier B.V. All rights reserved.
doi:10.1016/j.apcatb.2010.06.035

**Table 1**
Physicochemical properties of the catalysts.

| Catalysts | Metal loading (wt.%) | $S_{BET}$ ($m^2\ g^{-1}$) | $V_{pore}$ ($cm^3\ g^{-1}$) | $d_{pore}$ (nm) |
|---|---|---|---|---|
| $Ni/Al_2O_3$ | 20 | 124 | 0.96 | 21.5 |
| $Co/Al_2O_3$ | 20 | 118 | 0.95 | 21.5 |
| $Fe/Al_2O_3$ | 20 | 112 | 0.94 | 20.9 |
| $Cu/Al_2O_3$ | 20 | 115 | 0.96 | 21.8 |

acid reforming reaction also have not been checked in detail. Thus, catalytic behaviors of these four $Al_2O_3$-supported transition metals catalysts in steam reforming of acetic acid were studied in this study.

## 2. Experimental

### 2.1. Catalyst preparation

The supported catalysts with metal loading of 20 wt.% were prepared by incipient wetness impregnation method using the corresponding nitrate as the metal precursors. Before impregnation, the support γ-$Al_2O_3$ (129 $m^2$/g, 0.35–0.60 mm) was stabilized in air at 873 K for 6 h. After impregnation, the catalyst precursors were dried at room temperature for 24 h and and at 383 K for another 24 h. Finally, the catalyst precursors were calcined at 773 K for 4 h and the powders were crushed into particles with 0.20–0.56 mm in size for use. The BET specific area, volume of pores and average pore diameter of the prepared catalysts are listed in Table 1.

### 2.2. Catalytic activity measurements

Catalytic tests were carried out at atmospheric pressure in a fixed-bed continuous flow quartz reactor (i.d. 8 mm), consisting of a flow controller unit, a reactor unit, and an analysis unit. The reaction temperature increased from 573 to 873 K at a 50 K increment. The effluent gas and liquid products were taken for analysis after stabilizing for 1 h at each investigated temperature. Typically, 0.5 g catalyst diluted with equal amount of quartz was used in each run. Prior to the experiment, the calcined catalyst was reduced in situ at 873 K for 3 h (heating rate 10 K/min) with a 50 vol% $H_2/N_2$ mixture (flow rate 60 ml/min). The reaction mixture was fed into a pre-heater by a syringe pump with a liquid hourly space velocity (LHSV) of 8.3 $h^{-1}$ and a given steam to carbon ratio (S/C). The vaporized reaction mixture was fed into the reactor using $N_2$ (40 ml/min) as the carrier gas. The separation and quantification of the products were attained on two on-line chromatographs quipped with thermal-conductivity detectors (TCD) and flame ionization detectors (FID). Catalytic performance of a given catalyst was based on acetic acid conversion and $H_2$ selectivity. Acetic acid conversion was denoted as $X_{HAC}$ in the figures. $H_2$ selectivity was defined as the fraction of $H_2$ produced with respect to the theoretical full conversion of acetic acid to $H_2$ according to Eq. (1). The calculated method of the carbon-containing product's selectivity was similar to that of $H_2$.

$$S_{H_2}(\%) = 100 \times \frac{\text{moles of } H_2 \text{ production}}{\text{moles of acetic acid consumed} \times 4}.$$

$$S_{\text{carbon-containing product}}(\%) = 100 \times \frac{\text{moles of carbon-containing compounds}}{\text{moles of acetic acid consumed} \times 2}.$$

Liquid hourly space velocity (LHSV) was defined as volumetric flow rate of feed solution ($cm^3\ h^{-1}$))/(catalyst bed volume ($cm^3$)). Steam to carbon ratio (S/C) was defined by the formula: S/C = (moles of steam in the feed)/(moles of carbon in the feed):

$$CH_3COOH + 2H_2O \rightarrow 4H_2 + 2CO_2 \quad (\Delta H'_{298} = 131.4\,\text{kJ/mol}) \qquad (1)$$

### 2.3. Catalyst characterization

Temperature-programmed reduction analysis ($H_2$-TPR) was carried out by heating a sample (30 mg) from 298 to 1073 K at 20 K/min in a flow of 5 vol% $H_2$/Ar mixture (40 ml/min). The amount of $H_2$ consumed was measured by a TCD.

The X-ray diffraction spectra (XRD) measurements were performed on a Philips X pert MPD instrument using Cu Kα radiation in the scanning angle range of 10–80° at a scanning rate of 4°/min at 40 mA and 50 kV.

The amounts of carbon deposition on catalyst surface were analyzed by thermo-gravimetric analysis in a PerkinElmer TG/DTA apparatus (sensitivity: 0.2 mg). The catalyst was heated from room temperature to 1073 K. The ramp rate was 10 K/min and compressed air was used as the oxidant. The mass loss versus increasing temperature was measured. In the oxidation atmosphere, the oxidation of the metal in reduced catalyst might occur, which would result in weight gain and affect accuracy of results. In this case, the blank test of TG characterization over the freshly reduced metal catalysts will perform under the same conditions to deduct the weight gain from the oxidation of metals in catalysts.

## 3. Results and discussion

### 3.1. $H_2$-TPR characterizations

$H_2$-TPR characterization was conducted over the samples to understand reduction behaviors of the different metal oxides. The results are presented in Fig. 1. Cu oxide was easily reduced. A small shoulder and a sharp principal reduction peak in the low temperature region constituted the $H_2$-TPR profile of $Cu/Al_2O_3$ catalyst. In comparison, the reduction peaks of $Ni/Al_2O_3$, $Co/Al_2O_3$, and $Fe/Al_2O_3$ catalysts were much broader and appeared at higher temperatures. Nickel oxide in $Ni/Al_2O_3$ was difficult to be reduced under the reduction conditions employed. It could not be completely reduced even at the temperature as high as 1073 K. The $H_2$-TPR profile for $Co/Al_2O_3$ catalyst was composed of a principal peak at 733 K and a prolonged tail peak at 943 K, which were attributed to the reduction of $Co_3O_4$ to CoO and the subsequent reduction of CoO to metallic Co [37]. Fe oxide showed comparable reduction behavior with that of Co oxide. The peak centered at

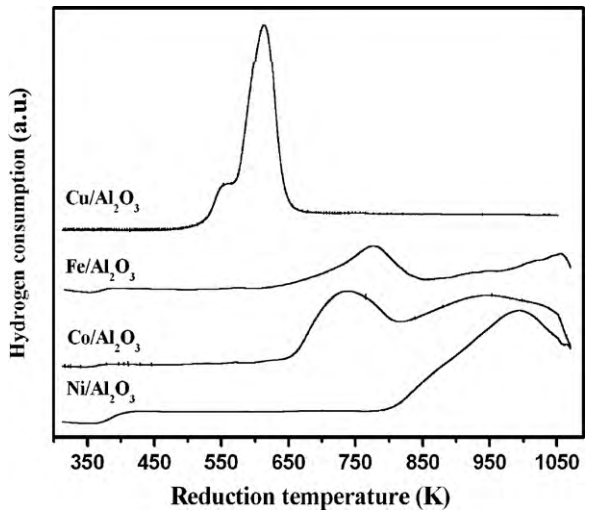


**Fig. 1.** $H_2$-TPR profiles for the $Al_2O_3$-supported catalysts.

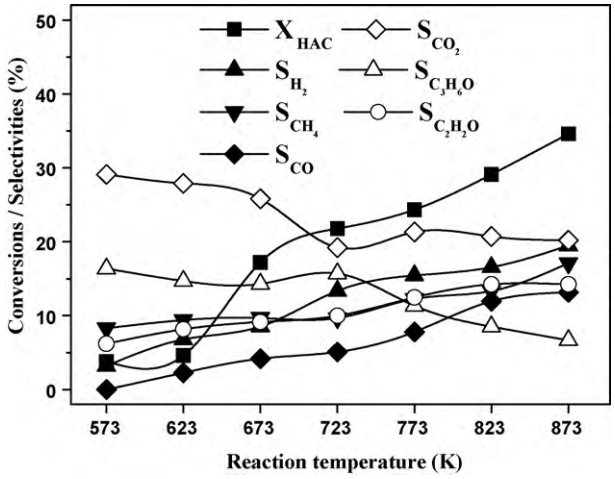


**Fig. 2.** Blank tests of steam reforming of acetic acid in the reactor filled with only quartz: S/C = 7.5; LHSV = 8.3 $h^{-1}$; $P$ = 1 atm.

776 K was assigned to the reduction of $Fe_2O_3$ to $Fe_3O_4$, while the high-temperature peak was related to the subsequent reduction of $Fe_3O_4$ to Fe, via FeO [38].

### 3.2. Evaluation of alumina-supported transition metal catalysts

Prior to performing catalytic reactions over the transition metal catalysts, the blank test in the reactor filled with only quartz was performed to measure the catalytic effect of quartz on acetic acid steam reforming. The catalytic results are presented in Fig. 2. Quartz showed some reforming activity under the reaction conditions. Acetic acid conversion near 35% and hydrogen selectivity near 20% were achieved at the maximum reaction temperature of 873 K. Nevertheless, in the low temperature regions, significant amounts of acetone and ketene were produced while the gaseous by-products, mainly $CH_4$ and CO, were produced in appreciable amounts in the high temperature regions. The organic by-products could not be further steam reformed over quartz with the increasing temperature.

Evaluation of the $M/Al_2O_3$ (M = Ni, Co, Fe or Cu) catalysts was subsequently conducted in the temperature region of 573–873 K. The catalytic behaviors of each catalyst at different temperatures are summarized in Figs. 3 and 4, where remarkable differences in terms of activity and product distributions could be observed. At 723 K, $Ni/Al_2O_3$ and $Co/Al_2O_3$ catalysts were able to convert acetic acid completely with selectivity toward hydrogen exceeding 90%. Whereas $Fe/Al_2O_3$ and $Cu/Al_2O_3$ catalysts showed negligible steam reforming activity. $CH_4$, acetone, and ketene were produced as the main products with only a small amount of $H_2$ was formed. The predominance of acetic acid decomposition [Eq. (2)], ketonization [Eq. (3)], and dehydration [Eq. (4)] reactions over $Fe/Al_2O_3$ and $Cu/Al_2O_3$ catalysts should be responsible for the production of the significant amounts of organic by-products:

$$CH_3COOH \rightarrow CH_4 + CO_2 \quad (\Delta H'_{298} = -33.5\,kJ\,mol^{-1}) \tag{2}$$

$$2CH_3COOH \rightarrow CH_3COCH_3 + CO_2 + H_2O\,(\Delta H'_{298} = 16.7\,kJ\,mol^{-1}) \tag{3}$$

$$CH_3COOH \rightarrow CH_2CO + H_2O \quad (\Delta H'_{298} = 131.9\,kJ\,mol^{-1}) \tag{4}$$

Reaction pathways for the products formation were significantly influenced by the nature of metallic phase. Steam reforming process involved cracking of both the C–C and C–H bonds in acetic

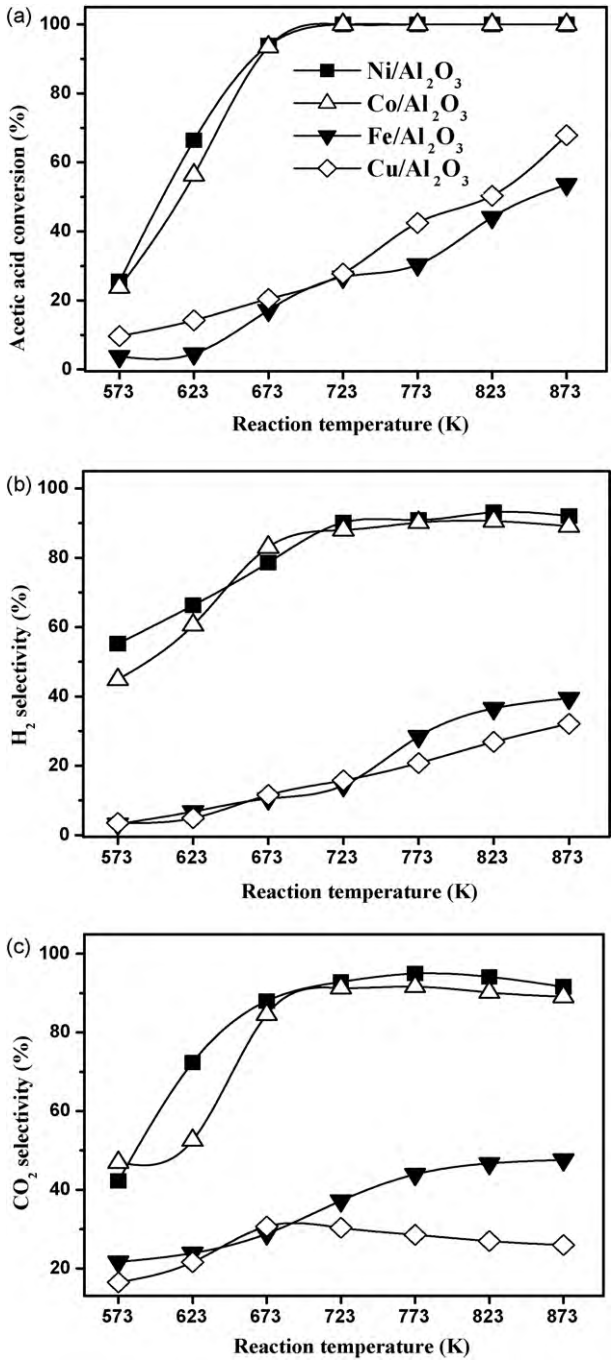


**Fig. 3.** Acetic acid conversions, $H_2$ and $CO_2$ selectivities versus reaction temperature: S/C = 7.5; LHSV = 8.3 $h^{-1}$; $P$ = 1 atm.

acid molecule on metal surface, forming the $CO_x$, $CH_x$, and $H_{ads}$ species. These intermediates were the precursors for the formation of CO, $CO_2$, and $H_2$ [24]. Therefore, a good performing catalyst should be active not only for the water gas shift reaction [Eq. (5)] to remove CO from metal surface, but also for the cleavage of C–C and C–H bonds to convert reactants and form hydrogen [39]. Ni, Co, and Fe, as Group VIII metals, showed high C–C bond breaking activity [40] and reasonable water–gas shift activity [41]. However, the experimental results showed that $Fe/Al_2O_3$ catalyst presented poor acetic acid reforming activity while $Ni/Al_2O_3$ and $Co/Al_2O_3$ catalysts performed much better. Fe species was much less active for the activation of C–H bond than Ni and Co species [42,43], which might be the main reason for its inferior catalytic activity for acetic

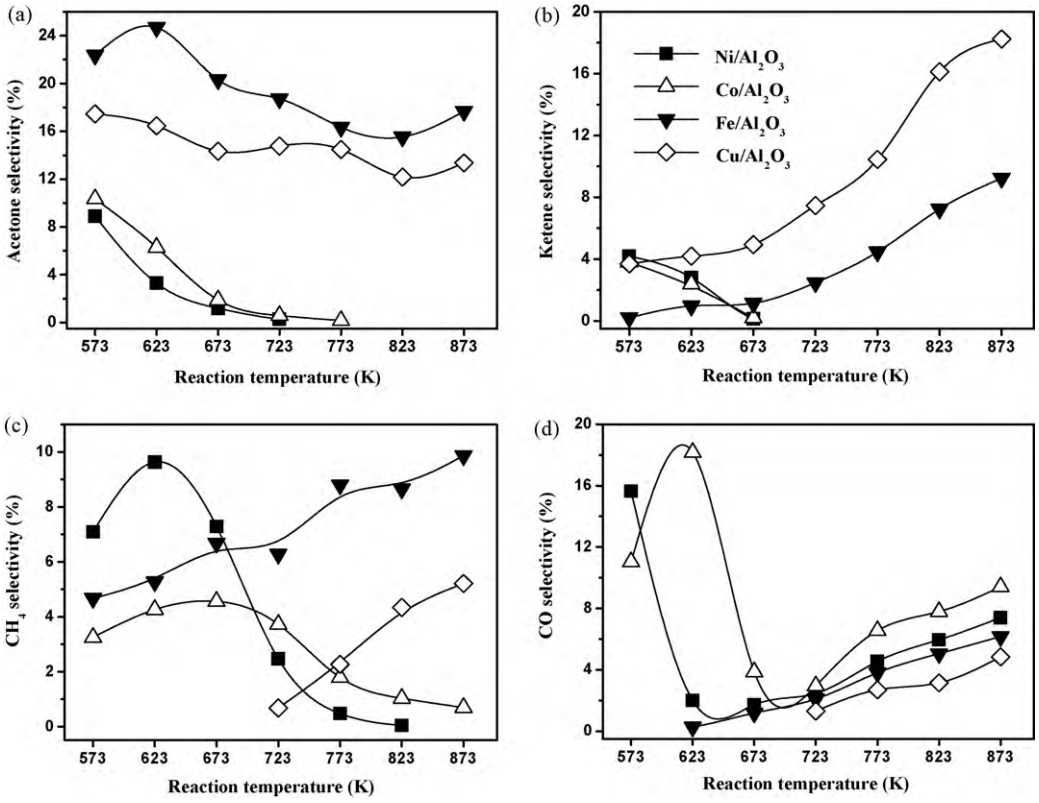


**Fig. 4.** Distribution of the by-products versus reaction temperature: S/C = 7.5; LHSV = 8.3 $h^{-1}$; $P$ = 1 atm.

acid conversion. As for the product distribution over $Fe/Al_2O_3$ catalyst, Fig. 4c shows a significant amount of $CH_4$ produced in the high temperature region, indicating that acetic acid decomposition reaction [Eq. (2)] occurred. The decomposition of acetic acid involved the cracking of C–C bond in acetic acid molecule, which might be promoted over $Fe/Al_2O_3$ catalyst. Furthermore, Fig. 4a shows a significant amount of acetone formed over $Fe/Al_2O_3$ catalyst, suggesting that the ketonization reaction was also promoted over $Fe/Al_2O_3$ catalyst. Although Cu showed good activity for the cleavage of C–H bond and much higher water gas shift activity than those of Group VIII metals [41], $Cu/Al_2O_3$ catalyst showed a very poor activity for acetic acid steam reforming. This was caused by the fact that Cu showed no activity for C–C bond cracking [40]. Thus, Cu was not an effective metal for steam reforming of the organic compound with C–C bond such as acetic acid. As shown in Fig. 4b, only the acetic acid dehydration reaction [Eq. (4)] was favored over $Cu/Al_2O_3$ catalyst.

$$CO + H_2O \rightarrow H_2 + CO_2 \quad (\Delta H'_{298} = -41.1\ \text{kJ mol}^{-1}) \tag{5}$$

### 3.3. Product distributions over $Ni/Al_2O_3$ and $Co/Al_2O_3$ catalysts at different temperatures

As presented above, the general catalytic performances of $Ni/Al_2O_3$ and $Co/Al_2O_3$ catalysts were comparable. However, some differences with respect to the distribution of the products such as the productions of CO and $CH_4$ over $Ni/Al_2O_3$ and $Co/Al_2O_3$ catalysts (see Fig. 4d and c) were observed. CO was an important intermediate and one of the main by-products in acetic acid reforming process. It was produced mainly via the decomposition of acetic acid [Eq. (6)] as well as the reverse water gas shift reactions [Eq. (7)] and eliminated by the water gas shift reaction [Eq. (5)] and the methanation reaction [Eq. (8)] [30,36]. As for $CH_4$, decomposition of acetic acid [Eq. (2)], methanation of carbon oxides [Eqs. (8) and (9)], and steam reforming of $CH_4$ [Eqs. (10) and (11)] were the main reactions determining its production in reforming process [36]:

$$CH_3COOH \rightarrow 2CO + 2H_2 \quad (\Delta H'_{298} = 213.7\ \text{kJ mol}^{-1}) \tag{6}$$

$$H_2 + CO_2 \rightarrow H_2O + CO \quad (\Delta H'_{298} = 41.1\ \text{kJ mol}^{-1}) \tag{7}$$

$$CO + 3H_2 \rightarrow CH_4 + H_2O \quad (\Delta H'_{298} = -206.1\ \text{kJ mol}^{-1}) \tag{8}$$

$$CO_2 + 4H_2 \rightarrow CH_4 + 2H_2O \quad (\Delta H'_{298} = -165.1\ \text{kJ mol}^{-1}) \tag{9}$$

$$CH_4 + 2H_2O \rightarrow CO_2 + 4H_2 \quad (\Delta H'_{298} = 165.1\ \text{kJ mol}^{-1}) \tag{10}$$

$$CH_4 + H_2O \rightarrow CO + 3H_2 \quad (\Delta H'_{298} = 206.1\ \text{kJ mol}^{-1}) \tag{11}$$

At the initial reaction temperatures, both $Ni/Al_2O_3$ and $Co/Al_2O_3$ catalysts gave high CO selectivity, which was probably induced by their low activity for the water gas shift reaction [Eq. (5)] due to the low reaction temperature. Nevertheless, at higher temperatures, the production of CO was more favorable over $Co/Al_2O_3$ catalyst. As for $CH_4$, its production was more favorable over $Ni/Al_2O_3$ catalyst at mild temperatures, but its amount decreased drastically to zero with the further increase of temperature to 823 K. In comparison, the amount of $CH_4$ over $Co/Al_2O_3$ catalyst was still appreciable at 873 K. The different activities of $Ni/Al_2O_3$ and $Co/Al_2O_3$ catalysts for the secondary reactions such as acetic acid decomposition, methanation, reverse water gas shift, or methane steam reforming reactions were speculated as the main reasons for their different CO and $CH_4$ selectivities.

Hence, additional experiments, including the acetic acid decomposition, methanation, and $CH_4$ steam reforming, were performed over $Ni/Al_2O_3$ and $Co/Al_2O_3$ catalysts, respectively. Acetic acid decomposition reaction was carried out over each catalyst at 673 K for 1 h using pure acetic acid with a LHSV of 5.0 $h^{-1}$. The results are presented in Fig. 5. Acetic acid conversions were comparable over Ni and Co catalysts, while the hydrogen yields over both are poor,

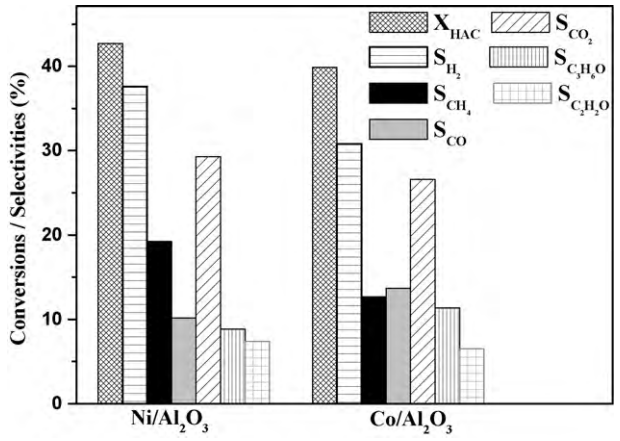


**Fig. 5.** Acetic acid conversions and product distribution over $Ni/Al_2O_3$ and $Co/Al_2O_3$ catalysts in acetic acid decomposition experiments: $T = 673$ K; LHSV = 5.0 $h^{-1}$; $P = 1$ atm.

due to the productions of significant amounts of $CH_4$, CO, acetone, and ketene. Nevertheless, different tendencies for the formations of $CH_4$ and CO over Ni and Co were observed. A higher $CH_4$ selectivity was obtained over $Ni/Al_2O_3$ catalyst while a higher CO selectivity was obtained over $Co/Al_2O_3$ catalyst. Evidently, $Ni/Al_2O_3$ catalyst was more selective to the decomposition of acetic acid to $CH_4$ and $CO_2$ [Eq. (2)] while $Co/Al_2O_3$ catalyst was more selective to the decomposition of acetic acid to CO and $H_2$ [Eq. (6)]. In addition, coke formation was detected in acetic acid decomposition tests. The coke formation rates over Ni and Co catalysts are 4.6 and 5.7 mgC/gCat/h, respectively.

The methanation reaction was performed over $Ni/Al_2O_3$ and $Co/Al_2O_3$ catalysts in the temperature region of 573–873 K using two reactors. Acetic acid was firstly reformed with steam in the first reactor to generate the effluent gas, which was then introduced into the second reactor to measure the methanation activity of the catalysts. Results are shown in Fig. 6. Both $Ni/Al_2O_3$ and $Co/Al_2O_3$ catalysts showed appreciable methanation activity. The production of $CH_4$ increased with increasing temperature and reached the maximum at 623 K. Further increasing temperature resulted in the decrease of $CH_4$ yield because of limitations of the thermodynamic equilibrium. Obviously, methanation of carbon oxides contributed to the formation of $CH_4$ in steam reforming, especially in the mild temperature region. The methanation reaction occurred with a higher rate over $Ni/Al_2O_3$ catalyst because of the higher $CH_4$ yields

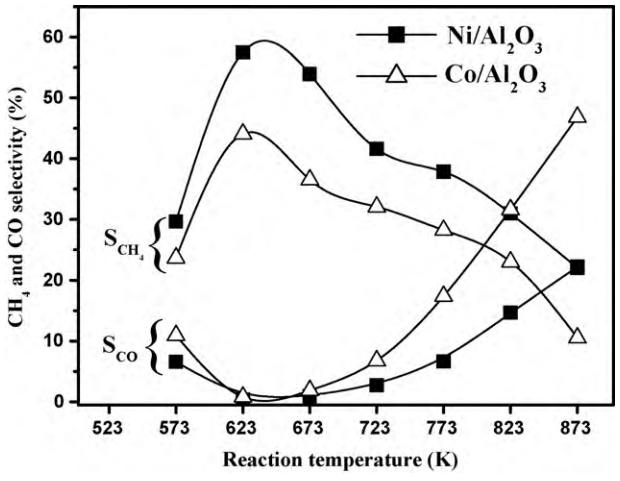


**Fig. 6.** Methanation reactions over $Ni/Al_2O_3$ and $Co/Al_2O_3$ catalysts: GHSV = 2400 $h^{-1}$; $P = 1$ atm.

obtained throughout the temperatures investigated. Therefore, at mild temperatures, the higher $CH_4$ selectivity over $Ni/Al_2O_3$ catalyst in acetic acid steam reforming could be related to the higher activities of $Ni/Al_2O_3$ catalyst for the methanation reaction and acetic acid decomposition reaction [Eq. (2)]. As for CO, the tendency for its production was almost converse with that of $CH_4$ versus the increasing temperature. CO selectivity decreased initially but then increased quickly with increasing temperature in the methanation reactions, indicating the occurrences of the methanation of CO [Eq. (8)] at lower temperatures and the reverse water gas shift reactions [Eq. (7)] at higher temperatures. CO methanation and the reverse water gas shift reactions were parallel in steam reforming process. Low temperature favored CO methanation to eliminate CO while high temperature favored the reverse water gas shift reaction to form CO. $Co/Al_2O_3$ catalyst was more selective toward the reverse water gas shift reaction than $Ni/Al_2O_3$ catalyst (see Fig. 6). Thus, the higher activities of $Co/Al_2O_3$ catalyst to the reverse water gas shift reaction and the acetic acid decomposition [Eq. (6)] resulted in the higher CO amounts in steam reforming process, as shown in Fig. 4d.

Steam reforming of methane was conducted over $Ni/Al_2O_3$ and $Co/Al_2O_3$ catalysts in the temperature region of 673–873 K with an S/C ratio of 4 and a GHSV of 7600 $h^{-1}$. $Ni/Al_2O_3$ catalyst was active at temperature above 723 K, whereas $Co/Al_2O_3$ showed negligible activity at the temperatures investigated (results were not shown). The high activity of $Ni/Al_2O_3$ catalyst for methane steam reforming should be responsible for the sharp decrease of $CH_4$ production above 773 K in acetic acid steam reforming (see Fig. 4c).

The experimental equilibrium of product distributions in catalytic reactions was affected by both catalytic performances of catalyst and experimental conditions employed. We compared the experimental results in terms of product distribution in this work with that predicted by the thermodynamic equilibrium in the work of Vagia and Lemonidou [44]. Lemonidou et al. conducted a thermodynamic analysis about steam reforming of acetic acid using the Aspen Plus 11.1 software under the assumed reaction conditions of temperature from 400 to 1300 K and steam to fuel ratio from 1 to 9. They predicted that acetic acid decomposition dominated at the initial reaction temperature (400 K), resulting in the formation of only $CH_4$ and $CO_2$ as the main products. Increasing temperature led to the decrease of both $CH_4$ and $CO_2$ production meanwhile the increase of $H_2$ production. However, further increase of reaction temperature to high temperature region led to the increase of CO concentration, which in turn decreased $H_2$ concentration to some extent. In our experiments, the results in the mild or high temperature region are very similar with that predicted by Lemonidou et al. Taking the $Ni/Al_2O_3$ catalyst for example, at 573 K and S/C of 7.5, the catalyst presented poor catalytic activity. In addition to $CH_4$ and $CO_2$ that were predicted by thermodynamic equilibrium, another two organic by-products, acetone and ketene, were also produced in appreciable amounts, which led to the low hydrogen yield. Increasing temperature remarkably promoted the efficiency of steam reforming. Hydrogen was produced as the main product in the mild temperature region meanwhile the productions of the by-products such as $CH_4$, acetone, and ketene decreased to a significant extent. It is probably that not only acetic acid but also the by-product such as $CH_4$, acetone, and ketene were steam reformed. However, further increase of temperature also led to the decrease of hydrogen production, due to the increase of CO selectivity at this stage. Taking the above results into consideration, it can be concluded that the tendency for the product composition versus reaction temperature is similar between our experimental results with that predicted with thermodynamic equilibrium by Lemonidou et al., although their reforming conditions were different from ours (temperature range: 573–873 K, S/C: 7.5).

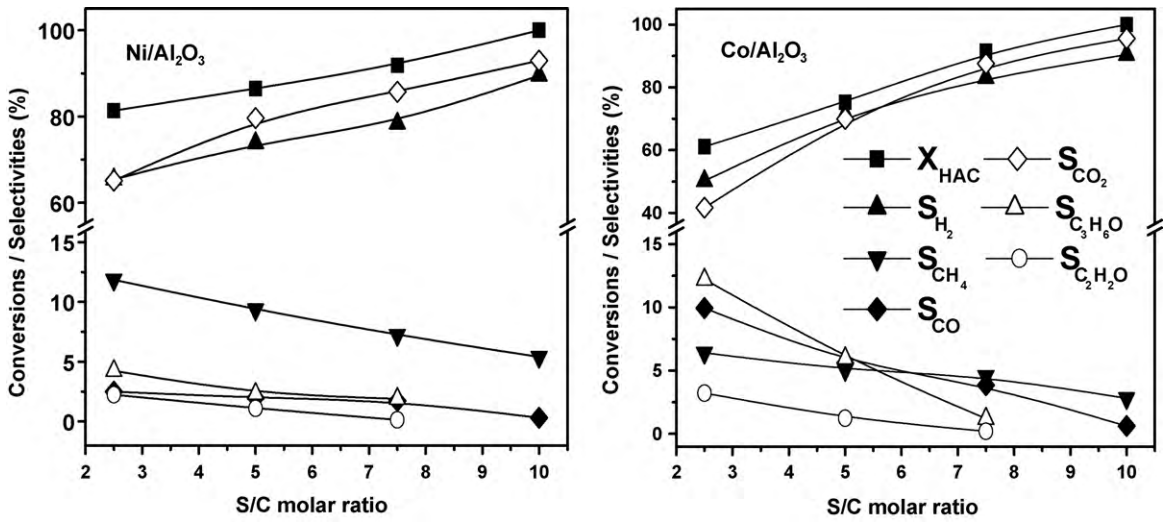


**Fig. 7.** Acetic acid conversions and product distributions of $Ni/Al_2O_3$ and $Co/Al_2O_3$ catalysts versus S/C ratio: $T = 673$ K; LHSV = 8.3 $h^{-1}$; $P = 1$ atm.

### 3.4. Catalytic behaviors of $Ni/Al_2O_3$ and $Co/Al_2O_3$ catalysts at different S/C ratios

Influences of S/C ratios on the catalytic performances of $Ni/Al_2O_3$ and $Co/Al_2O_3$ catalysts were investigated at 673 K. Results are given in Fig. 7. Acetic acid conversion and $H_2$ selectivity decreased monotonously with the decrease of S/C ratios over either $Ni/Al_2O_3$ or $Co/Al_2O_3$ catalyst. Low steam ratios in reactants resulted in low steam reforming rates [21] and significant amounts of by-products. However, it seemed that the impact of the low S/C ratios on $Co/Al_2O_3$ catalyst was more significant, since much lower acetic acid conversion and much more by-products such as CO and acetone were obtained. In comparison, the decrease of acetic acid conversion and $H_2$ yield were much mild over $Ni/Al_2O_3$ catalyst versus the decreasing steam ratios, indicating the higher tolerance of $Ni/Al_2O_3$ catalyst toward the low S/C ratios. Furthermore, $Ni/Al_2O_3$ catalyst also presented superior activity for water gas shift reaction [Eq. (5)] to remove CO. The CO selectivity was much lower over $Ni/Al_2O_3$ catalyst than over $Co/Al_2O_3$ catalyst even at the low S/C ratios of 2.5. However, the production of $CH_4$ was more significant over $Ni/Al_2O_3$ catalyst, which could be related to the higher activity of $Ni/Al_2O_3$ catalyst for acetic acid decomposition [Eq. (2)] and methanation reactions [Eqs. (8) and (9)]. As for the routes for methane formation under this low S/C, acetic acid decomposition reaction [Eq. (2)] was supposed to be the main pathway, since it was favored at low steam ratios. In another aspect, the lower steam reforming efficiency at the low S/C ratios resulted in lower $H_2$ and $CO_2$ yields, which was unfavorable for the occurrence of methanation reactions. In industry, the steam reforming reaction generally was conducted at lower S/C ratios, which was more energy-efficient due to the less water needed to be evaporated. In this sense, $Ni/Al_2O_3$ catalyst is more practical in application in industry due to its high tolerance toward the low steam ratios in reactants.

### 3.5. Catalytic behaviors of $Ni/Al_2O_3$ and $Co/Al_2O_3$ catalysts in long-term stability tests

Developing stable catalysts is one of the major issues in steam reforming reactions [45,46]. To assess the stability of $Ni/Al_2O_3$ and $Co/Al_2O_3$ catalysts, endurance tests were performed at 673 K and S/C of 7.5 for 100 h. Results are presented in Fig. 8. $Ni/Al_2O_3$ catalyst exhibited rather stable catalytic behaviors in the whole time on stream. Conversely, $Co/Al_2O_3$ catalyst deactivated drastically after

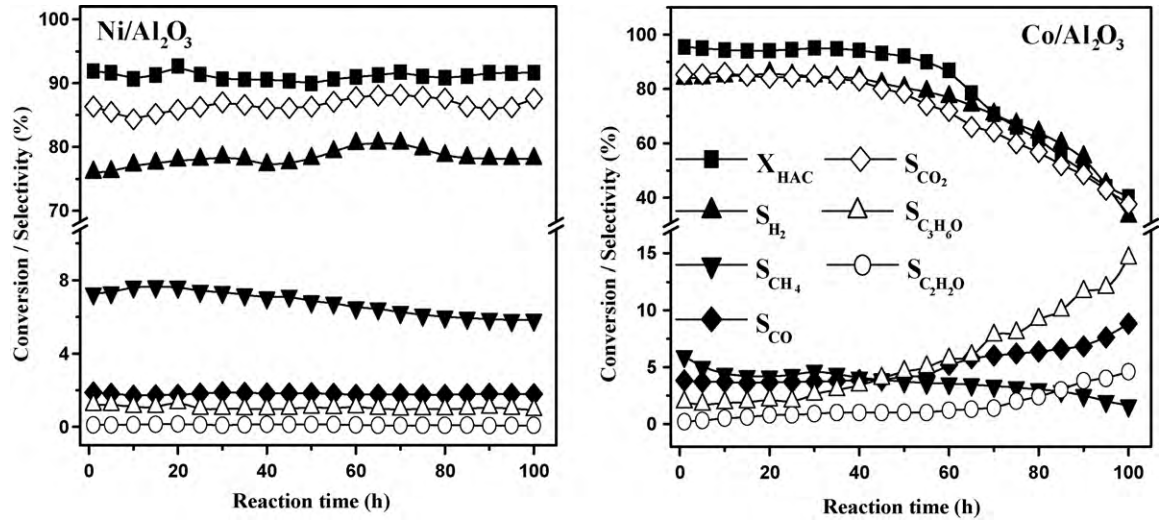


**Fig. 8.** Stability tests of $Ni/Al_2O_3$ and $Co/Al_2O_3$ catalysts: T = 673 K; S/C = 7.5; LHSV = 8.3 $h^{-1}$; $P = 1$ atm.

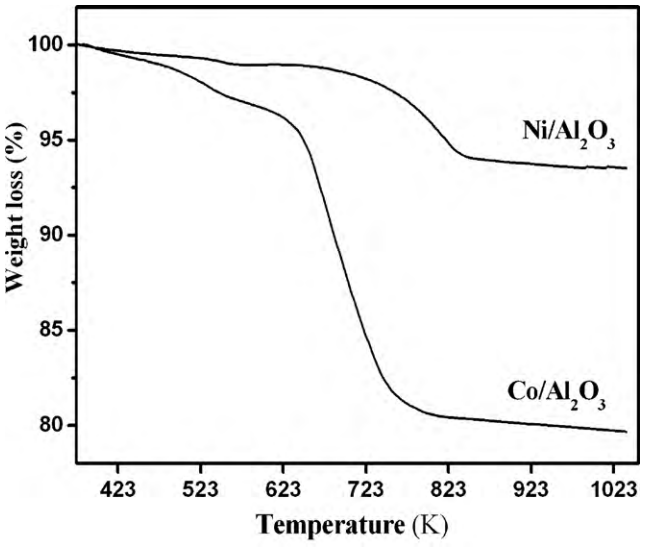


**Fig. 9.** TG results of the endurance-tested $Ni/Al_2O_3$ and $Co/Al_2O_3$ catalysts.

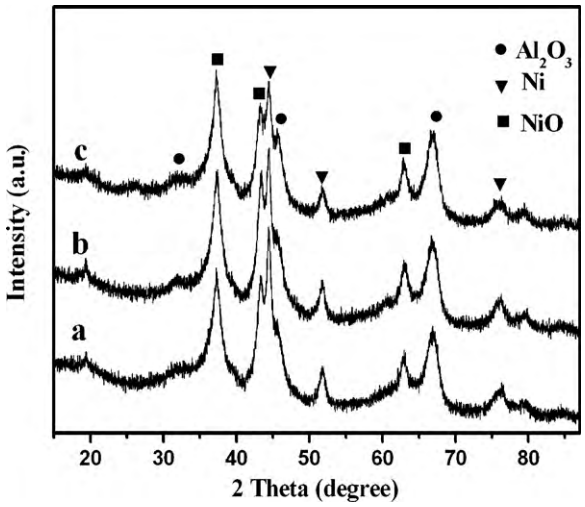


**Fig. 10.** XRD patterns for $Ni/Al_2O_3$ catalyst after different treatment. a: The reduced catalyst; b: the used catalyst; c: the endurance-tested catalyst.

50 h of time on stream and lost more than 50% of its initial activity at the end of the test. Significant amounts of by-products except $CH_4$ generated along with the prolonged reaction time, leading to sharp decrease of $H_2$ yield. Reforming catalysts are generally subject to several deactivation mechanisms including coking, sintering, and oxidation of the metallic phase, which result in the decrease of the active metal sites on catalyst surface and lower catalyst ability to convert hydrocarbon to $C_1$ products and $H_2$ [47]. To understand the deactivation mechanisms of Co catalyst, TG and XRD characterizations were conducted over not only Co catalysts but also Ni catalysts for comparison. Results of TG measurements shown in Fig. 9 indicated that the coke formation occurred with a much higher rate over $Co/Al_2O_3$ catalyst than over $Ni/Al_2O_3$ catalyst. The large amount of coke might come from the decomposition of acetic acid [Eq. (12)], the Boudouard reaction [Eq. (13)], or the polymerization of acetone [Eq. (14)] [48]. Decomposition of acetic acid was not thermodynamically favored under the reforming conditions employed because of the existence of excess steam [44]. Thus, the Boudouard reaction and the polymerized acetone were supposed as important routes for coke formation, since both Boudouard reaction and acetone polymerization reaction were favored at the mild temperature employed in the endurance tests [49,48]. Moreover, the amounts of CO and acetone over $Co/Al_2O_3$ catalyst were appreciable in the initial reaction time and increased significantly at the end of the endurance test. In converse, the carbon deposition over $Ni/Al_2O_3$ catalyst was much mild. The production of CO was also mild, while acetone presented only in a trace amount throughout the endurance test.

$$CH_3COOH \rightarrow C + CO_2 + 2H_2 \quad (\Delta H'_{298} = 41.3\,kJ\,mol^{-1}) \tag{12}$$

$$2CO \rightarrow C + CO_2 \quad (\Delta H'_{298} = -172.4\,kJ\,mol^{-1}) \tag{13}$$

$$CH_3COCH_3 \rightarrow \text{oligomerization} \rightarrow \text{carbon deposits} \tag{14}$$

XRD characterizations were conducted over Ni and Co catalysts after endurance tests (endurance-tested catalyst) to identify the structure reconstructions of the samples and sintering of the metals after the long-term stability tests. Results are given in Figs. 10 and 11, respectively. For comparison, XRD results of the freshly reduced and used catalysts were also presented. Here the reduced catalyst was the catalyst reduced at 873 K for 3 h (heating rate 10 K/min) with a 50 vol% $H_2/N_2$ mixture (flow rate 60 ml/min) and cooled to room temperature in a nitrogen stream. The used catalyst was the catalyst tested under the conditions: S/C = 7.5, LHSV = 8.3 $h^{-1}$, and temperature from 573 to 873 K. For $Ni/Al_2O_3$ catalyst, the reduced, used, and endurance-tested samples exhibited comparable diffraction patterns. The characteristic diffractions of Ni, NiO, and $Al_2O_3$ phases were observed. The observation of the NiO phase in the reduced, used, and endurance-tested catalysts was in accordance with the $H_2$-TPR results that nickel oxides could not be completely reduced under the reduction conditions employed. Besides, the metallic Ni crystal grain sizes calculated by the Scherrer formula in the reduced and endurance-tested catalysts were 20 and 22 nm, respectively. Obviously, no remarkable metal sintering of $Ni/Al_2O_3$ catalyst occurred in the endurance test. The catalyst had stable internal structure. For $Co/Al_2O_3$ catalyst, its crystal phases practically differed after the different treatments. In the freshly reduced sample, only metallic Co phase was visible. While for the used catalyst, in addition to metallic Co, the characteristic diffractions of both CoO and $Co_3O_4$ phases were observed, implying the oxidization of part metallic Co species during the steam reforming process. As for the endurance-tested Co catalyst, the metallic phase practically disappeared, only the crystal phases of cobalt oxides, $Co_3O_4$ and CoO, were visible. Obviously, the oxidation of metallic Co in the long-term reforming process was serious. In addition, the diffraction intensity of $Co_3O_4$ phase in the endurance-tested

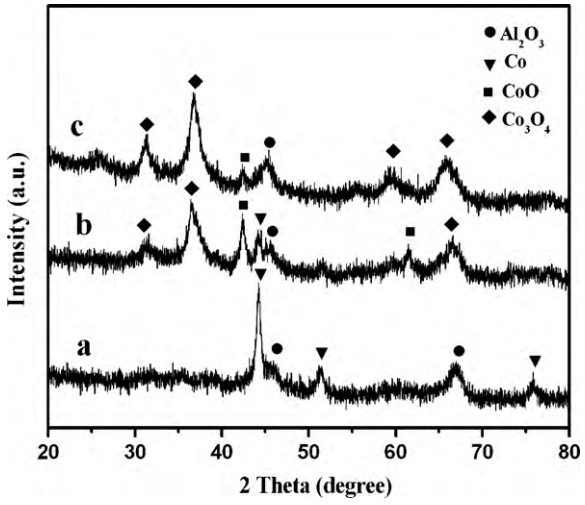


**Fig. 11.** XRD patterns for $Co/Al_2O_3$ catalyst after different treatment. a: The reduced catalyst; b: the used catalyst; c: the endurance-tested catalyst.

catalyst increased remarkably at the expense of the diffraction of CoO phase, which provided a good evidence for the subsequent oxidation of some Co (II) to Co (III) species. The oxidation of Co catalyst in catalytic reactions also has been reported by other group [48,50], which resulted from its exposure to excess steam at elevated temperature and would lead to significant catalyst deactivation.

The oxidation of metallic Co and the serious coke deposition would inevitably result in the decrease of the active sites on catalyst surface. The less active sites were probably unfavorable for the occurrences of methanation or decomposition reactions [Eq. (2)], since the deactivation of $Co/Al_2O_3$ catalyst was accompanied by the linearly decrease of $CH_4$ selectivity (see Fig. 8). In comparison, the generations of acetone and ketene were not affected. On the contrary, acetone and ketene amounts increased substantially after the deactivation of Co catalyst, indicating that the ketonization and dehydration reactions were not catalyzed by the metallic sites, and they probably were catalyzed by the acidic sites of the alumina support.

### 3.6. Comparison of the catalytic performances of Ni catalysts in acetic acid reforming reaction

Ni catalyst is a traditional reforming catalyst and it showed much better reforming activity and stability than other transition metals investigated in this paper, as the catalytic results presented above. Therefore, we further compared the catalytic performances of our Ni catalyst with other Ni catalyst systems employed in acetic acid reforming reactions in terms of catalytic activity and hydrogen selectivity. There are quite a few published works dealing with acetic acid steam reforming by employing the Ni catalysts with different catalysts formulation. In these works, two strategies were generally applied to improve the catalytic activity of Ni catalysts: optimization of the preparation methods and the modification of Ni with promoters or supports.

Bilbao and co-workers [26] investigated acetic acid reforming using a Ni–Al catalyst prepared by co-precipitation method at 923 K and S/C of 5.58. The catalyst was active and selective under these conditions. A hydrogen yield of 0.119 g/g acetic acid was obtained. The hydrogen selectivity with this hydrogen yield, which was calculated with the method referred in our work, was about 89.2%. This value was similar with the hydrogen selectivity of 90.7% achieved over $Ni/Al_2O_3$ catalyst in this study at 723 K and S/C of 7.5. Garcia and co-workers [51] also studied acetic acid reforming over both the bare and Ca promoted Ni/Al catalysts, which were prepared also by the co-precipitation method, under the reforming conditions similar with that of Bilbao and co-workers [26]. The bare Ni/Al catalyst presents similar activity and hydrogen selectivity with that of Bilbao and co-workers [26], and the addition of Ca did not result in an improvement in catalytic performance. In another work [27], they studied the effects of Ni loading on catalytic performances. The Ni/Al catalyst with Ni loading of 28% presented superior catalytic activity and selectivity. Hydrogen selectivity reached 88.5% at 923 K, which is much higher than that over the catalysts with Ni loading of 23% ($S_{H_2}$ : 67.5%) or 33% ($S_{H_2}$ : 46.5%). Basagiannis and Verykios [30] investigated acetic acid steam reforming over a $Ni/Al_2O_3$ catalyst prepared by impregnation method at high temperatures with a $H_2O$/HAc molar ratio of 3. The catalyst showed significant activity above 1023 K, where acetic acid was completely converted and hydrogen selectivity almost attained 100%. The modification of $Ni/Al_2O_3$ with La did not result in a remarkable increase of both activity and hydrogen selectivity, while the addition of Mg drastically shifted the temperature required for complete conversion of acetic acid to 923 K or lower. Vagia and Lemonidou et al. [52] also studied acetic acid steam reforming over a Ca modified $Ni/Al_2O_3$ catalyst at S/C of 3, The 5 wt.% $Ni/CaO{\cdot}2Al_2O_3$ catalyst present superior catalytic performances. At 923 K, full conversion of acetic acid is attained with hydrogen yield of almost 90%. Here the hydrogen yield defined by the author is similar with the hydrogen selectivity defined in our work. In another work [53], they developed a $Ni/CeO_2$–$ZrO_2$ catalyst and found that it was as active and selective as the Ca modified catalyst. Seshan and co-workers [54] also investigated the supporting effect on catalytic behaviors of Ni catalyst at 973 K and S/C of 5. They found that the $Ni/ZrO_2$, Ni/K–$ZrO_2$, Ni/La–$ZrO_2$, and Ni/K–La–$ZrO_2$ catalysts showed comparable initial catalytic performance in terms of acetic acid conversion (100%) and hydrogen yields (ca. 87%).

As the results presented above, although the formulations of Ni catalysts are similar, distinct catalytic behaviors are observed. The preparation method, pre-treatment procedures, promoters, supports, as well as the experimental conditions employed should be responsible for the different catalytic activity, selectivity, and stability of Ni catalysts in steam reforming reactions. The preparation method significantly affects the interaction of Ni species with support, which further affects the metal dispersion, metal particle size, and metal sintering rate at high temperatures and then the catalytic performance. The pre-treatment procedures mainly refer to the calcination and reduction conditions, which will affect the reduction degree of Ni species, or rather, the number of the active metal sites presented on catalyst surface. The nature of promoter and support, similarly with that of preparation method, affects the interaction of metal with support and also the reducibility of Ni species, which further affects the dispersion of active metal sites on catalyst surface. Furthermore, the promoter and support may have synergistic effect with Ni species or even directly participated in catalytic reactions, which may change the reaction pathways in reforming process. The experimental conditions such as reaction temperature, space velocity, and S/C will affect the adsorption and activation of the reactants on catalyst surface, which further affects the product distribution. Furthermore, the reaction condition also affects the secondary reactions between the primary reforming products and then the final product distributions. Although there have been plenty of works contributed to the preparation and application of Ni-based catalysts in different catalytic reactions, the further research on how to further improve the catalytic activity, selectivity and especially the stability of Ni catalyst is still necessary.

## 4. Conclusion

Results presented above clearly indicated that:

(1) $Ni/Al_2O_3$ and $Co/Al_2O_3$ catalysts were highly active and selective for hydrogen production, while the activity of $Fe/Al_2O_3$ and $Cu/Al_2O_3$ catalysts for steam reforming of acetic acid was low. These distinct catalytic behaviors could be related to the different activities of the metallic phases for cracking the chemical bonds of acetic acid molecule. Ni and Co species not only were active for cracking of C–C bond, but also for C–H bond, while Fe species was only active for the activation of C–C bond and Cu was only active for the cracking of C–H bond.

(2) $Co/Al_2O_3$ catalyst was more active for the reverse water gas shift reaction and the decomposition of acetic acid to CO, leading to higher CO amounts in reforming process. In comparison, $Ni/Al_2O_3$ catalyst was more active for methanation reactions and the decomposition of acetic acid to $CH_4$, leading to higher $CH_4$ amounts at mild temperatures. While at high reaction temperatures, the amount of $CH_4$ over $Ni/Al_2O_3$ catalyst was in trace level because of the high activity of $Ni/Al_2O_3$ catalyst for $CH_4$ steam reforming. Besides, compared with $Co/Al_2O_3$ catalyst, $Ni/Al_2O_3$ catalyst was more tolerable toward the low S/C ratios. Superior steam reforming activity and $H_2$ selectivity was still achieved under the harsh experimental conditions.

(3) Under the same reaction conditions, $Ni/Al_2O_3$ catalyst was far more stable than $Co/Al_2O_3$ catalyst. The serious coke deposition and oxidation of the active metal resulted in the fast deactivation of $Co/Al_2O_3$ catalyst. In converse, much slower carbon deposition, metal sintering rate, and much higher resistivity to the oxidation of metallic Ni guaranteed the stable catalytic performances of $Ni/Al_2O_3$ catalyst.

## Acknowledgement

We acknowledge the financial support of the 973 Project of China (Nos. 2007CB210204, 2007CB613305, and 2009CB220003).

## References

[1] S. Huang, P. Ganesan, B.N. Popov, Appl. Catal. B: Environ. 96 (2010) 224.
[2] E. Antolini, Appl. Catal. B: Environ. 88 (2009) 1.
[3] J.A. Torres, J. Llorca, A. Casanovas, M. Domınguez, J. Salvado, D. Montane, J. Power Sources 169 (2007) 158.
[4] K.D. Beard, J.W.V. Zee, J.R. Monnier, Appl. Catal. B: Environ. 88 (2009) 185.
[5] S. Huang, P. Ganesan, B.N. Popov, Appl. Catal. B: Environ. 93 (2009) 75.
[6] G. Avgouropoulos, J. Papavasiliou, M.K. Daletou, J.K. Kallitsis, T. Ioannides, S. Neophytides, Appl. Catal. B: Environ. 90 (2009) 628.
[7] Z. Wang, Y. Pan, T. Dong, X. Zhu, T. Kan, L. Yuan, Y. Torimoto, M. Sadakata, Q. Li, Appl. Catal. A: Gen. 320 (2007) 24.
[8] P. Ciambelli, V. Palma, A. Ruggiero, Appl. Catal. B: Environ. 96 (2010) 190.
[9] F.M. Mercader, M.J. Groeneveld, S.R.A. Kersten, N.W.J. Way, C.J. Schaverien, J.A. Hogendoorn, Appl. Catal. B: Environ. 96 (2010) 57.
[10] Y. Shinmi, S. Koso, T. Kubota, Y. Nakagawa, K. Tomishige, Appl. Catal. B: Environ. 94 (2010) 318.
[11] X. Hu, G. Lu, Catal. Commun. 10 (2009) 1633.
[12] E.I. Gurbuz, E.L. Kunkes, J.A. Dumesic, Appl. Catal. B: Environ. 94 (2010) 134.
[13] C. Rioche, S. Kulkarni, F.C. Meunier, J.P. Breen, R. Burch, Appl. Catal. B: Environ. 61 (2005) 130.
[14] I. Graca, F.R. Ribeiro, H.S. Cerqueira, Y.L. Lam, M.B.B. Almeida, Appl. Catal. B: Environ. 90 (2009) 556.
[15] X. Hu, G. Lu, Appl. Catal. B: Environ. 88 (2009) 376.
[16] G. Fogassy, N. Thegarid, G. Toussaint, A.C. van Veen, Y. Schuurman, C. Mirodatos, Appl. Catal. B: Environ. 96 (2010) 476.
[17] H.J. Park, H.S. Heo, J. Jeon, J. Kim, R. Ryoo, K. Jeong, Y. Park, Appl. Catal. B: Environ. 95 (2010) 365.
[18] R. Nava, B. Pawelec, P. Castano, M.C. Alvarez-Galvan, C.V. Loricera, J.L.G. Fierro, Appl. Catal. B: Environ. 92 (2009) 154.
[19] L. Garcia, R. French, S. Czernik, E. Chornet, Appl. Catal. A: Gen. 201 (2000) 225.
[20] C. Branca, P. Giudicianni, C.D. Blasi, Ind. Eng. Chem. Res. 42 (2003) 3190.
[21] M. Marquevich, S. Czernik, E. Chornet, D. Montane, Energy Fuels 13 (1999) 1160.
[22] X. Hu, G. Lu, Energy Fuels 23 (2009) 926.
[23] D. Wang, S. Czernik, D. Montane, M. Mann, E. Chornet, Ind. Eng. Chem. Res. 36 (1997) 1507.
[24] D. Wang, D. Montane, E. Chornet, Appl. Catal. A: Gen. 143 (1996) 245.
[25] X. Hu, G. Lu, Chem. Lett. 37 (2008) 614.
[26] J.R. Galdamez, L. Garcia, R. Bilbao, Energy Fuels 19 (2005) 1133.
[27] F. Bimbela, M. Oliva, J. Ruiz, L. García, J. Arauzo, J. Anal. Appl. Pyrol. 79 (2007) 112.
[28] X. Hu, G. Lu, Green Chem. 11 (2009) 724.
[29] A.C. Basagiannis, X.E. Verykios, Appl. Catal. A: Gen. 308 (2006) 182.
[30] A.C. Basagiannis, X.E. Verykios, Int. J. Hydrogen Energy 32 (2007) 3343.
[31] A.C. Basagiannis, X.E. Verykios, Catal. Today 127 (2007) 256.
[32] K. Takanabe, K. Aika, K. Seshan, L. Lefferts, J. Catal. 227 (2004) 101.
[33] K. Takanabe, K. Aika, K. Inazu, T. Baba, K. Seshan, L. Lefferts, J. Catal. 243 (2006) 263.
[34] K. Takanabe, K. Aika, K. Seshan, L. Lefferts, Chem. Eng. J. 120 (2006) 133.
[35] X. Hu, G. Lu, Chem. Lett. 35 (2006) 452.
[36] X. Hu, G. Lu, J. Mol. Catal. A: Chem. 261 (2007) 43.
[37] M.S. Batista, R.K.S. Santos, E.M. Assaf, J.M. Assaf, E.A. Ticianelli, J. Power Sources 134 (2004) 27.
[38] M.S. Batista, M. Wallau, E.A. Urquieta-Gonzalez, Braz. J. Chem. Eng. 22 (2005) 441.
[39] R.R. Davda, J.W. Shabaker, G.W. Huber, R.D. Cortright, J.A. Dumesic, Appl. Catal. B: Environ. 43 (2003) 13.
[40] J.H. Sinfelt, Adv. Catal. 23 (1973) 91.
[41] D.C. Grenoble, M.M. Estadt, D.F. Ollis, J. Catal. 67 (1981) 90.
[42] U.K. Singh, M.A. Vannice, J. Catal. 199 (2001) 73.
[43] Y. Schuurman, V. Ducarme, T. Chen, W. Li, C. Mirodatos, G.A. Martin, Appl. Catal. A: Gen. 163 (1997) 227.
[44] E.C. Vagia, A.A. Lemonidou, Int. J. Hydrogen Energy 32 (2007) 212.
[45] S. Xu, X. Wang, Fuel 84 (2005) 563.
[46] N. Laosiripojana, W. Sangtongkitcharoen, S. Assabumrungrat, Fuel 85 (2006) 323.
[47] J. Sehested, J. Catal. 217 (2003) 417.
[48] B. Zhang, X. Tang, Y. Li, W. Cai, Y. Xu, W. Shen, Catal. Commun. 7 (2006) 367.
[49] D.L. Trimm, Catal. Today 49 (1999) 3.
[50] S. Freni, S. Cavallaro, N. Mondello, L. Spadaro, F. Frusteri, Catal. Commun. 4 (2003) 259.
[51] J.A. Medrano, M. Oliva, J. Ruiz, L. Garcia, J. Arauzo, Int. J. Hydrogen Energy 33 (2008) 4387.
[52] E.C. Vagia, A.A. Lemonidou, Appl. Catal. A: Gen. 351 (2008) 111.
[53] E.C. Vagia, A.A. Lemonidou, J. Catal. 269 (2010) 388.
[54] B.M. Guell, I.M.T. Silva, K. Seshan, L. Lefferts, Appl. Catal. B: Environ. 88 (2009) 59.